보건학석사 학위논문

Anti-obesity effect of *Bacteroides vulgatus* via improvement of gut microbiome dysbiosis and intestinal barrier function

박테로이데스 불가투스 균주의 장내 미생물 불균형 회복과 장벽 기능 개선 및 항 비만 효과 연구

2019년 11월

서울대학교 보건대학원

환경보건학과 환경보건학 전공

김 진 욱

Anti-obesity effect of *Bacteroides vulgatus* via improvement of gut microbiome dysbiosis and intestinal barrier function

박테로이데스 불가투스 균주의 장내 미생물 불균형 회복과 장벽 기능 개선 및 항 비만 효과 연구

지도교수 고 광 표

이 논문을 보건학석사 학위논문으로 제출함

2019년 11월

서울대학교 보건대학원

환경보건학과 환경보건학 전공

김 진 욱

김진욱의 보건학석사 학위논문을 인준함

2019년 12월

위 원 장 김 성 균 (인)

부 위 원 장 유 현 주 (인)

위 원 고 광 표 (인)

Abstract

Anti-obesity effect of *Bacteroides vulgatus* via improvement of gut microbiome dysbiosis and intestinal barrier function

Kim Jin Wook

Dept. of Environmental Health

The Graduate School of Public Health

Seoul National University

Gut microbiome is an important factor modulating immune and metabolic dysfunctions in development of obesity. As two dominant phyla in the human gut microbiome, the *Firmicutes* to *Bacteroidetes* ratio (F/B ratio) has been known as a microbial biomarker representing the obese status of host. Although the significant correlation between

abundances of *Bacteroides* sp. and host obesity has been reported in many clinical and animal studies, the causal effect and related mechanisms of *Bacteroides* sp. on regulating obesity is not clear. In this study, we isolated *Bacteroides vulgatus* (BV SNUG40005) from healthy human fecal specimens and investigated the effect on weight gain and glucose intolerance in a high fat diet (HFD)-induced obesity mouse model. Bacterial strain was daily administered by oral gavage for 17 weeks ($1X10^9$ CFU/mouse/day) and continued until the end of the experiments. The diet-induced obesity model, mice were fed high-fat diet from 0 day to the end of the experiments. The BV SNUG40005 significantly reduced weight gain, glucose intolerance, adipose tissue weight, and metabolic inflammation. We observed mice administered BV SNUG40005 increased cecal microbial diversity and reshape community structure compared with HFD control group. Furthermore, BV SNUG40005 administration increased the inner mucus layer thickness and the expression levels of related genes (*Muc2, Muc4, Muc13, Klf4*) in colon tissues. Furthermore, BV SNUG40005 significantly increased tight junction related gene (*Zo-1*) in human epithelial Caco-2 cells, and mucus production related genes (*Muc2, Muc4, Muc13, Klf4*) in human goblet-like LS174T cells. Taken together,

BV SNUG40005 successfully alleviated obesity and metabolic disorder and can be applied to a microbiome-based therapy for obesity.

Key words: *Bacteroides vulgatus*, Obesity, Diet-induced Obesity Mice, Type II diabetes, Glucose intolerance, Mucus layer, Tight junction, Microbiome

Student No. 2018-28883

CONTENTS

List of Tables

List of Figures

List of Abbreviations

Diet induced Obesity (DIO)

Firmicutes to *Bacteroidetes* ratio (F/B ratio)

Ribosomal RNA (rRNA)

Weight / Volume (w/v)

Volume / Volume (v/v)

Phosphate buffer saline (PBS)

Colony Forming Unit (CFU)

High Fat Diet (HFD)

Normal Diet (ND)

Hight Fat Diet with *Bacteroides vulgatus* (HFDB)

Normal Diet with *Bacteroides vulgatus* (NDB)

Isolated *Bacteroides vulgatus* (BV SNUG40005)

Gonadal white adipose tissue (GWAT)

Hematoxylin and Eosin stain (H&E)

Intraperitoneal glucose intolerance test (IPGTT)

Lipopolysaccharides (LPS)

Enzyme-linked immunosorbent assay (ELISA)

Polymerase chain reaction (PCR)

4′,6-Diamidino-2-Phenylindole (DAPI)

Quantitative Insights into Microbial Ecology (QIIME)

Operational taxonomic units (OTUs)

Principle coordinate analysis (PCoA)

Dulbecco′s Modified Eagle′s Medium (DMEM)

Hydroxyethyl piperazine Ethane Sulfonic acid (HEPES)

Standard error of the mean (SEM)

Analysis of variance (ANOVA)

Interleukin (IL)

Toll – like receptors (TLRs)

mammalian target of rapamycin (mTOR)

Wheat germ agglutinin (WGA)

Fetal bovine serum (FBS)

Regenerating islet-derived protein III- *gamma* (Reg3g*)*

Zonula occludens-1 (ZO-1)

Pathogen-associated molecular patterns (PAMPs)

Mucin (MUC)

Acetylsalicylic acid (ASA)

Kruppel-like factor 4 (KLF4)

Interferon regulatory factor 4 (IRF4)

I. Introduction

Obesity is an emerging global disease in the 21st century, with more than 2 billion people worldwide and a dangerous disease of 3 million deaths per year.[1] Furthermore, obesity is known to contribute to the development of various diseases such as atherosclerosis, high blood pressure, diabetes, and cancer, which is a very important disease for health.[2-4] Most obese patients have chronic metabolic syndrome, which undermines the homeostasis of metabolic processes in the body, further accelerating disease development. Metabolic syndrome can also lead to chronic inflammatory reactions, which can lead to a variety of complications due to loss of function of the immune system.[5, 6] Obesity also affects the intestinal epithelial environment and microbiota. An unbalanced diet or intake of biased nutrients results in colonic decay of the intestinal microbes, resulting in more obesity due to negative feedback.[7, 8] And the imbalance of gut microbiota known as dysbiosis, leads to the alteration of the intestinal epithelial inner mucosal layer and permeability. It also can promote inflammation by modulating cytokine activity.[9, 10]

For this reason, the effects of obesity on the intestinal microbiota and the improvement of obesity using intestinal microorganisms are being

actively studied around the world.[11]

Among them, *Firmicutes* to *Bacteroidetes* ratio (F / B Ratio) using *Firmicutes* and *Bacteroidetes,* which are most representative of intestinal microbial community, is widely known as a biomarker of intestinal microorganisms indicating the degree of obesity in patients. High levels of *Bacteroidetes* are detected in normal people, while *Firmicutes* are high in obese patients.[12, 13]

Bacteroides spp. are early colonizing bacteria in the mammalian gut and are known to shape and direct the host immune system and metabolic activities.[14] *Bacteroides* species also regulate host physiology via immune systems.[15]

Various probiotic products on the market are known to have anti-obesity effects by increasing the growth rate of *Bacteroidetes* when ingested with probiotic strains.[16] However, probiotics strains do not colonize successfully in the intestine even if ingested, most of them are washed away, so long-term effects are difficult to expect.[17]

Nevertheless, no studies have demonstrated the effect on obesity when directly treated with *Bacteroidetes* strains. Therefore, it is necessary to investigate whether the direct treatment of the *Bacteroidetes* strain

against obesity increases the proportion of *Bacteroidetes* in the intestinal microbiome and affects weight loss.

In this study, we isolated BV SNUG40005 from healthy, moderately weighted adult Korean fecal samples. Using this strain, we hypothesize that when BV SNUG40005 from human were treated in obese mice, they settled normally in the intestine, alleviated the imbalance of the intestinal microbiota, and gave the positive effect on metabolic syndrome as obesity. Furthermore, we hypothesize that BV SNUG40005 will have a positive effect on obesity relief by not only changing the microbiome structure but also mucus secretion and tight junction.

II. Materials and Methods

1. Bacterial strain preparation

BV SNUG40005 were isolated from fecal samples of healthy Korean adult feces. All isolates were identified to the species level by sequencing of 16S rRNA and EzBioCloud's Identify Service (http://www.Ezbiocloud.net). Frozen stock of BV SNUG40005 was thawed and inoculated on Chocolate agar (3.3%; w/v, MB cell) agar containing Sheep Blood Defibrinated (7%; w/v, MB cell), Growth Factor Mixture (1%; w/v, MB cell), L-cysteine (0.05%; w/v; Sigma-aldrich) and incubated at 37℃ for 48 hours in anaerobic condition. 2 times of subculture (1% v/v) of incubation subsequently followed for activation of bacterial culture. The number of cfu of BV SNUG40005 strain was determined by measuring LIVE/DEAD™ BacLight™ Bacterial Viability and Counting Kit (Invitrogen, L34856), for flow cytometry (BD Accuri ™ C6 Plus flow cytometry, BD Biosciences, San Jose, CA, USA). For oral inoculation of the mice, bacteria grown for 24hr were subcultured for 12hr, were washed two times with sterile PBS to a concentration of 2 x 10^9/ml PBS. 200μl of this daily-prepared suspension were administrated by oral gavage every day, whereas the controls received 200μl of PBS via the same procedure.

2. Animals

Female C57BL/6J mice (6-week-old) were obtained from Central Lab Animal Inc. (Republic of Korea) and maintained under specific pathogen–free (SPF) conditions at the Institute for Experimental Animals, College of Medicine, Seoul National University. After one week of adaptation, the mice were divided into four groups (ND, NDB, HFD, HFDB) and treated with ampicillin (1 g/L) in drinking water for a week to reduce colonization by *Bacteroides* species.

Two groups of mice were fed HFD (HFD and HFDB, 60% fat; n=16; Research Diets-D12492). And to compare the fecal microbiota with the HFD group, the other two groups of mice were fed ND (ND and NDB, 10% fat; n=16; Research Diets-D12450B). The BV SNUG40005, prepared daily, was administered by oral gavage at 2.0 x 10^9 cfu per mouse (HFDB and NDB groups, n=8, respectively). Food intake and body weight were measured once per week. Fecal samples were collected at 5 time points (before antibiotic treatment, before BV SNUG40005 administration, and at 5 days, 9 weeks, and 18 weeks after administration). At week 16, an intraperitoneal glucose tolerance test was conducted. At week 18, the mice were sacrificed, and tissues (colon, cecum, and gonadal fat) were collected and stored at -80°C before

analysis. Blood samples were obtained by cardiac puncture under isoflurane anesthesia. Thirty minutes after blood clotting at RT, the serum was separated by centrifugation (2,000 x g, 10 min, 4°C). The supernatant (serum) was transferred into a 1.5-mL tube and stored at -80°C until use. Mouse experimental scheme are shown in Figure 1. Experimental procedures were reviewed and approved by the Institutional Animal Care and Usage Committee of Seoul National University.

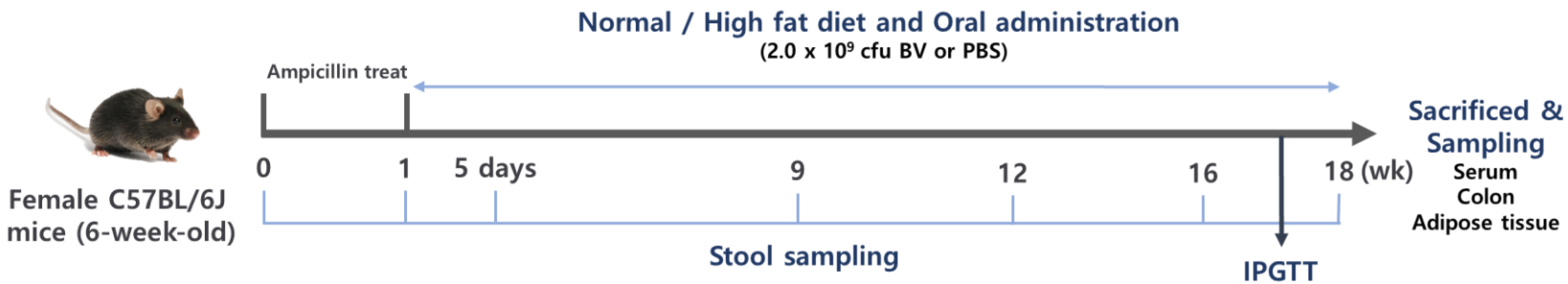

Figure 1. Experimental scheme of high-fat diet induced obesity mouse models

(A) Experimental scheme of 18-weeks diet-induced obesity mouse model. Mice were treated with ampicillin (1 g/L) in drinking water for a week. Mice were divided into four groups: High fat diet fed with PBS-administered group (HFD), High fat diet fed with BV-administered group (HFDB), Normal fat diet fed with PBS-administered group (ND), Normal fat diet fed with BV-administered group (NDB). PBS-administered group administered PBS by oral gavage, BV-administered group administered BV SNUG40005 by oral gavage at 2.0 x 10^9 cfu per mouse. All mice are fed high fat diet from 0 day to end of the experiment. Stool samples are collected at before and after antibiotics treatment, 5 days, 9 weeks, 12 weeks, 16 weeks and 18 weeks. At week 16, an intraperitoneal glucose tolerance test was conducted. At week 18, the mice were sacrificed, and tissues (colon, serum, and gonadal fat) were collected.

3. Measurement of weight change and adipose tissue weight

The body weight of each mouse was measured once a week during the trial, after which the mice were anesthetized. Weight change calculates the rate of increase in weight based on the weight of each mouse at 0 week.

The adipose tissue weights are collected GWAT at sacrifices, measured on a balance, and compared between groups.

4. Isolation of Colon and Adipose tissue

Mice were sacrificed by CO_2 asphyxiation followed by cervical dislocation, and sections of the distal colon were collected and placed in cassettes. Tissues were fixed by immersion in methacarn solution (60% methanol, 30% chloroform, 10% acetic acid) for 48 h, followed by two successive washes each in methanol for 30 min, ethanol for 20 min, and xylene for 15 min.[18] Tissue samples within cassettes were then submerged in melted paraffin at 68 °C for 1 h, removed, and kept at room temperature until sectioning. Paraffin blocks were cut into 4 μm-thick sections and deparaffinized for immunofluorescence. And adipose tissues were fixed in formalin (Sigma Aldrich, MO, USA). Adipose tissue sections were stained with hematoxylin and eosin stain (H&E) for general morphology of adipose cell.

5. Glucose intolerance test

At week 16, an intraperitoneal glucose tolerance test was conducted. Plasma glucose concentration measured during intraperitoneal glucose intolerance test (IPGTT) for C57Bl/6J mice fed a high-fat-diet with administered BV SNUG40005 or PBS. Before the experiment, feed is starved for 16 hours to check for fasting blood glucose. Calculate the desired glucose dose based on the each mouse weight (2mg/kg).[19] Blood glucose level were measured at 6 time points (before injected glucose, after injected glucose, and at 15min, 30 min, 60 min, and 90 min after injection). Blood glucose concentrations were measured on an Accu-Chek® Performa, blood glucose meter.

6. Determination of serum LPS and Insulin

Blood was collected by cardiac puncture immediately after mice were anaesthetised by isoflurane (Hana Pharm Co., Ltd., Republic of Korea). The blood was coagulated for 30 minutes at room temperature and centrifuged subsequently at 13,000 g for 5 minutes. Collected serum was stored at -80°C until further analysis. Ultra Sensitive Mouse Insulin ELISA Kit (Crystal Chem, IL, USA) was used to quantify the Insulin levels in serum. Mouse Lipopolysaccharides (LPS) ELISA Kit (CUSABIO, TX, USA) was used to quantify the LPS levels in serum. The assay was performed according to the manufacturer's instructions.

7. Real-time PCR

RNA was isolated from colon tissue and cell line using easy-spin™ [DNA free] Total RNA extraction Kit (iNtRON Biotechnology, Republic of Korea). Complementary DNA (cDNA) was synthesized using High-Capacity cDNA Reverse Transcription Kit (Thermo Fisher Scientific, MA, USA). Synthesized cDNA was used to perform quantitative PCR with Power SYBR® Green Master Mix (Thermo Fisher Scientific, MA USA) on the Applied Biosystems™ QuantStudio™ 6 Flex Real-Time PCR System (Applied Biosystems, MA, USA). Mouse primers sequences are shown in Table 1, And human primers sequences are shown in Table 2.

Table 1. Mouse PCR primers

Mouse Gene	Sequence (5'→3')
GAPDH	Fw: GCA CAG TCA AGG CCG AGA AT
	Rw: GCC TTC TCC ATG GTG GTG AA
IL-6	Fw: TAG TCC TTC CTA CCC CAA TTT CC
	Rw: TTG GTC CTT AGC CAC TCC TTC
TNFa	Fw: CCC AGG TAT ATG GGC TCA TAC C
	Rw: GCC GAT TTG CTA TCT CAT ACC AGG
F4/80	Fw: TTT CCT CGC CTG CTT CTT C
	Rw: CCC CGT CTC TGT ATT CAA CC
mTOR	Fw: CCA ATG AGA GGA AGG GTG GCA TC
	Rw: GGA CGC CAT TTC CAT GAC AAC TG
Muc1	Fw: CCC TAC CTA CCA CAC TCA CGG ACG
	Rw: GTG GTC ACC ACA GCT GGG TTG GTA
Muc2	Fw: GCT GAC GAG TGG TTG GTG AAT G
	Rw: GAT GAG GTG GCA GAC AGG AGA C
Muc4	Fw: GAG GGC TAC TGT CAC AAT GGA GGC
	Rw: AGG GTT CCG AAG AGG ATC CCG TAG
Muc13	Fw: GCC AGT CCT CCC ACC ACG GTA
	Rw: CTG GGA CCT GTG CTT CCA CCG
Klf4	Fw: AGC CAC CCA CAC TTG TGA CTA TG
	Rw: CAG TGG TAA GGT TTC TCG CCT GTG
Irf4	Fw: TGC AAG CTC TTT GAC ACA CA
	Rw: CAA AGC ACA GAG TCA CCT GG
Zo-1	Fw: CCA CCT CTG TCC AGC TCT TC
	Rw: CAC CGG AGT GAT GGT TTT CT

Occludin	Fw: CCT CCA ATG GCA AAG TGA AT
	Rw: CTC CCC ACC TGT CGT GTA GT
Claudin4	Fw: ACT TTT TGT GGT CAC CGA CT
	Rw: GCG AGC ATC GAG TCG TAC AT
Reg3 γ	Fw: CCA TCT TCA CGT AGC AGC
	Rw: CAA GAT GTC CTG AGG GC
IL-22	Fw: TGG TGC CTT TCC TGA CCA AA
	Rw: TCT GGA TGT TCT GGT CGT CAC
IL-23	Fw: AAC AGC TTA AGG ATG CCC AGG TTC
	Rw: ATA ATG GTG TCC TTG CCC TTC ACG
IL-25	Fw: TGG CAA TGA TCG TGG GAA CC
	Rw: GAG AGA TGG CCC TGC TGT TGA

Fw represents sequences of a forward primer

Rw represents sequences of a reverse primer

Table 2. Human PCR primers

Human Gene	Sequence (5'→3')
GAPDH	Fw: GAA GGT GAA GGT CGG AGT C
	Rw: GAA GAT GGT GAT GGG ATT TC
Muc2	Fw: CTG CAC CAA GAC CGT CCT CAT G
	Rw: GCA AGG ACT GAA CAA AGA CTC AGA
Muc4	Fw: AGG CGT TCT TAT ACC ACG TTC
	Rw: TGT AGC CAT CGC ATC TGA AG
Klf4	Fw: AGA GGA GCC CAA GCC AAA GA
	Rw: CAG TCA CAG TGG TAA GGT TTC TC
Zo-1	Fw: CGG TCC TCT GAG CCT GTA AG
	Rw: GGA TCT ACA TGC GAC GAC AA
Occludin4	Fw: TCA GGG AAT ATC CAC CTA TCA CTT CAG
	Rw: CAT CAG CAG CAG CCA TGT ACT CTT CAC
Claudin	Fw: AGC CTT CCA GGT CCT CAA CT
	Rw: AGC AGC GAG TCG TAC ACC TT

Fw represents sequences of a forward primer

Rw represents sequences of a reverse primer

8. Colon tissue preparation and visualizing

Thin (4-µm-thick) cross-sections of Carnoy's fixed distal colon segments were stained with DAPI for DNA, and with Alexafluor-633 conjugated wheat germ agglutinin (WGA-Alexa633, Invitrogen, MA, USA) to visualize mucins. Slides were mounted using ProLong™ Diamond Antifade Mountant with DAPI (Invitrogen, MA USA) to preserve fluorescence.[20] Staining procedure followed by *Preservation of mucus in histological sections* (Johansson and Hansson, 2012)[18]. Mucus structure was visualized using Leica SP5 laser scanning microscope (Leica Microsystems, Mannheim, Germany).

9. Intestinal microbiota and predicted community metagenomic analysis

Total genomic DNA from cecum contents was extracted using QIAmp Fast DNA stool mini kit (Qiagen, Hilden, Germany). The V4 region of 16S rRNA gene was amplified using the barcoded primers 515F and 806R. The concentration and fragment size of PCR amplicons purified using QIAquick PCR Purification Kit (Qiagen, Hilden, Germany). Raw FASTQ files were demultiplexed and quality filtered and data was processed by using Quantitative Insights into Microbial Ecology (QIIME) 1.8.0 software (http://qiime.org/). The sequences were clustered into operational taxonomic units (OTUs) at least 97% identity and the relative abundances of microbial taxa genus to kingdom were generated from nonrarefied OTU table. Alpha-diversity index (Chao1 index) was estimated for significant differences among groups. Beta diversity was calculated using the UniFrac distance between samples and visualized in two-dimensional (2D) plots based on weighted principle coordinate analysis (PCoA). In addition, by comparing the groups, the Gini index was calculated to identify which specific strains had the greatest difference in order.

10. Colon epithelial cell line

Human colon epithelial cells (Caco-2 ATCC® HTB-37™, LS174T (ATCC® CL188™) were obtained from the American Type Culture Collection. Cells were cultured in DMEM (Gibco, Paisley, UK) culture medium containing with 1% penicillin/streptomycin, 1% gentamycin, 10mM HEPES, 1.5% sodium bicarbonate and 10% Fetal bovine serum (FBS) and were counted with a hemocytometer. Cell viability was checked with trypan blue staining under the microscope. BV SNUG40005 were treated to grown cell, the Bacteria: Cell ratio was 100:1 and incubated in 6 well plates (SPL, Republic of Korea) at 37°C for 24 hours. After 24 hours, the cells were collected and lysed. mRNA was extracted using easy-spin™ [DNA free] Total RNA extraction Kit (iNtRON Biotechnology, Republic of Korea) and complementary DNA (cDNA) was synthesized subsequently using High-Capacity cDNA Reverse Transcription Kit (Thermo Fisher Scientific, MA, USA).

11. Statistical analysis

Differences between each group were compared using unpaired Student's t-test, as appropriate, or one-way analysis of variance (ANOVA) (version 8.0, GraphPad software, San Diego, CA). All values were expressed as means±standard error of the mean (SEM). Statistical difference was accepted at $p<0.05$.

III. Results

1. BV SNUG40005 alleviated obesity in a DIO mouse model induced by high-fat diet.

To assess the anti-obesity effect of BV SNUG40005 in *In-vivo*, 6-week-old mice maintained antibiotic drinking water for 1 week to adjust the abundance of *Bacteroidetes*. All groups were given HFD for the next 18 weeks, and BV SNUG40005 and PBS were orally administered to each mouse at a concentration of 2×10^9 cfu/mouse. When comparing the BV-administered mice and the PBS-administered mice, it is apparent that the BV-administered mice lost weight (Fig. 2A). The weight was measured at weekly intervals, and when comparing the weight of the last 18 weeks, it can be seen that the group of mice administered BV SNUG40005 significantly reduced the weight (Fig. 2B). When comparing the weight during 18 weeks, the effect of BV SNUG40005 began to be seen from the 4th week, and showed a significant difference in the weight from the 6th week, and the difference gradually increased (Fig. 2C). To compare the differences more precisely, the weight changes were compared based on the weight of 0 week. When comparing WC at week 18, very significant differences were observed in BV-administered groups (Fig. 2D). Comparing WC for 18 weeks, as with weight, effects began to

appear at 4 weeks, and significant at 6 weeks, further increasing (Fig. 2E). Through this, BV SNUG40005 was administered to the DIO mouse model, the anti-obesity effect in the mouse can be observed through the change in weight.

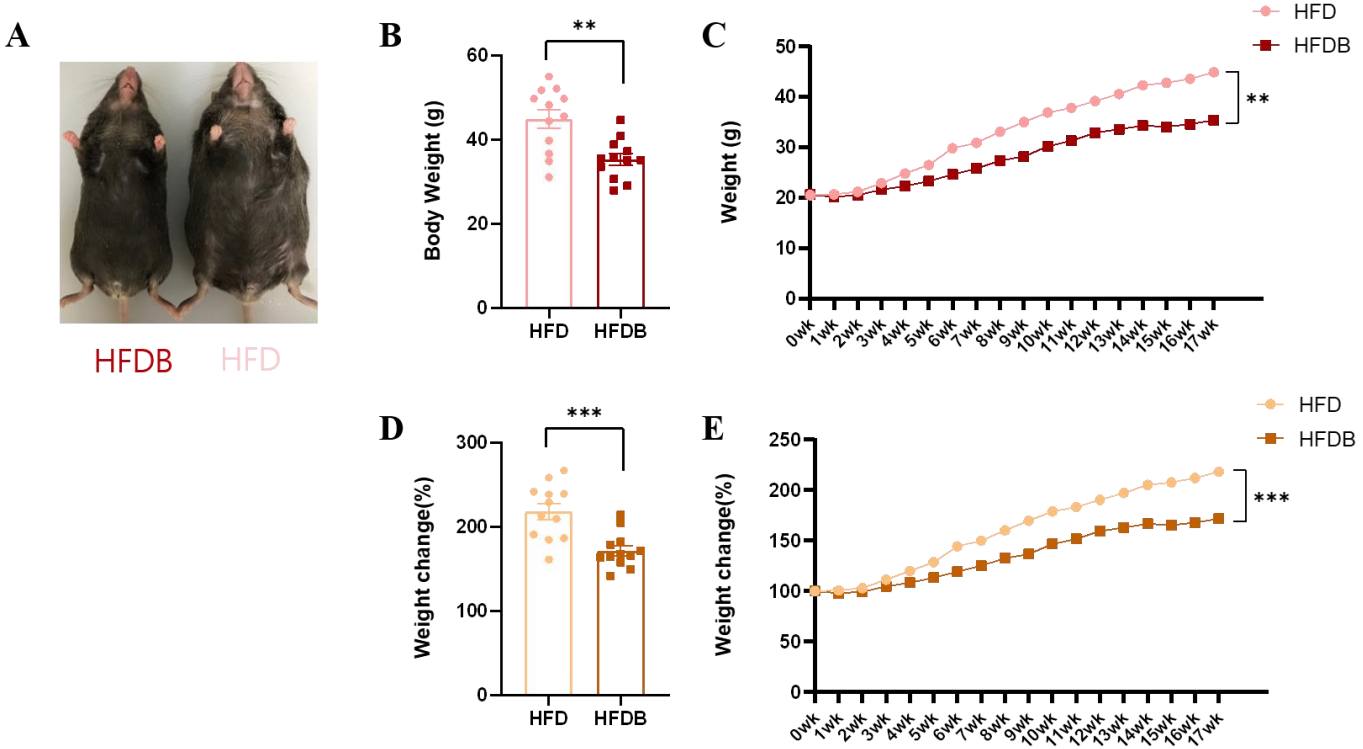
A
HFDB
HFD
B
Body Weight (g)
60
40
20
0
**
HFD
HFDB
C
Weight (g)
50
40
30
20
10
0
**
HFD
HFDB
0wk
1wk
2wk
3wk
4wk
5wk
6wk
7wk
8wk
9wk
10wk
11wk
12wk
13wk
14wk
15wk
16wk
17wk
D
Weight change(%)
300
200
100
0
***
HFD
HFDB
E
Weight change(%)
250
200
150
100
50
0
***
HFD
HFDB

Figure 2. BV SNUG40005 alleviated weight and weight change in a DIO mouse model induced by high-fat diet.

All groups were given HFD for the next 18 weeks, and BV SNUG40005 and PBS were orally administered to each mouse at a concentration of 2×10^9 cfu/mouse. A phenotype of the mouse is a picture of a typical mouse at 18 weeks, weight was measured at the same time each week. (A) State of mouse of the 18th week, (B) Weight of individual mice between groups at week 18, (C) Changes in mean mouse weights between groups of mice over 18 weeks, (D) Weight change of individual mice between groups at week 18, (E) Changes in mean mouse weight change between groups of mice over 18 weeks. Each value represents each mouse. Statistical analysis was performed using a one-tailed unpaired t test based on 12 mice per group and error bars represent SEM. *, $P < 0.05$; **, $P < 0.01$; ***, $P < 0.001$.

2. BV SNUG40005 reduced adipose tissue weight and inflammation.

To determine the changes in body fat in BV-administered mice, we compared the weight of gonadal adipose tissues after sacrifice, and to compare inflammation-related markers, RNA was extracted from adipose tissue and gene expression was confirmed by real-time qPCR. First, at sacrifice, adipose tissue was obtained and fixed in 10% formalin, and Adipose tissue sections were stained with hematoxylin and eosin stain (H&E) for general morphology of adipose cell. And it was confirmed that the size of the adipose cells was decreased in the group of mice administered BV SNUG40005 (Fig. 3A). To determine the reduction in body fat in BV-administered mice, the weight of both Gonadal white adipose tissues at the time of sacrifice was measured, and the weight of GWAT in the BV-administered group was significantly reduced when compared to the PBS-administered group (Fig. 3B). We assessed the mRNA expression of inflammation related genes to examine the effect of BV SNUG40005 on anti-inflammatory efficacy in adipose tissue from obesity. When the pro-inflammatory cytokine IL-6 and TNFa were compared, a decreasing tendency was observed in the BV SNUG40005 administration group. To assess the differentiation of macrophage, comparing the expression of F4 / 80, it can be seen that significantly decreased in the BV SNUG40005 administration group.

And the expression of mTOR involved in the secretion of pro-inflammatory cytokines, a decreasing tendency was observed in the BV SNUG40005 administration group (Fig. 3C).

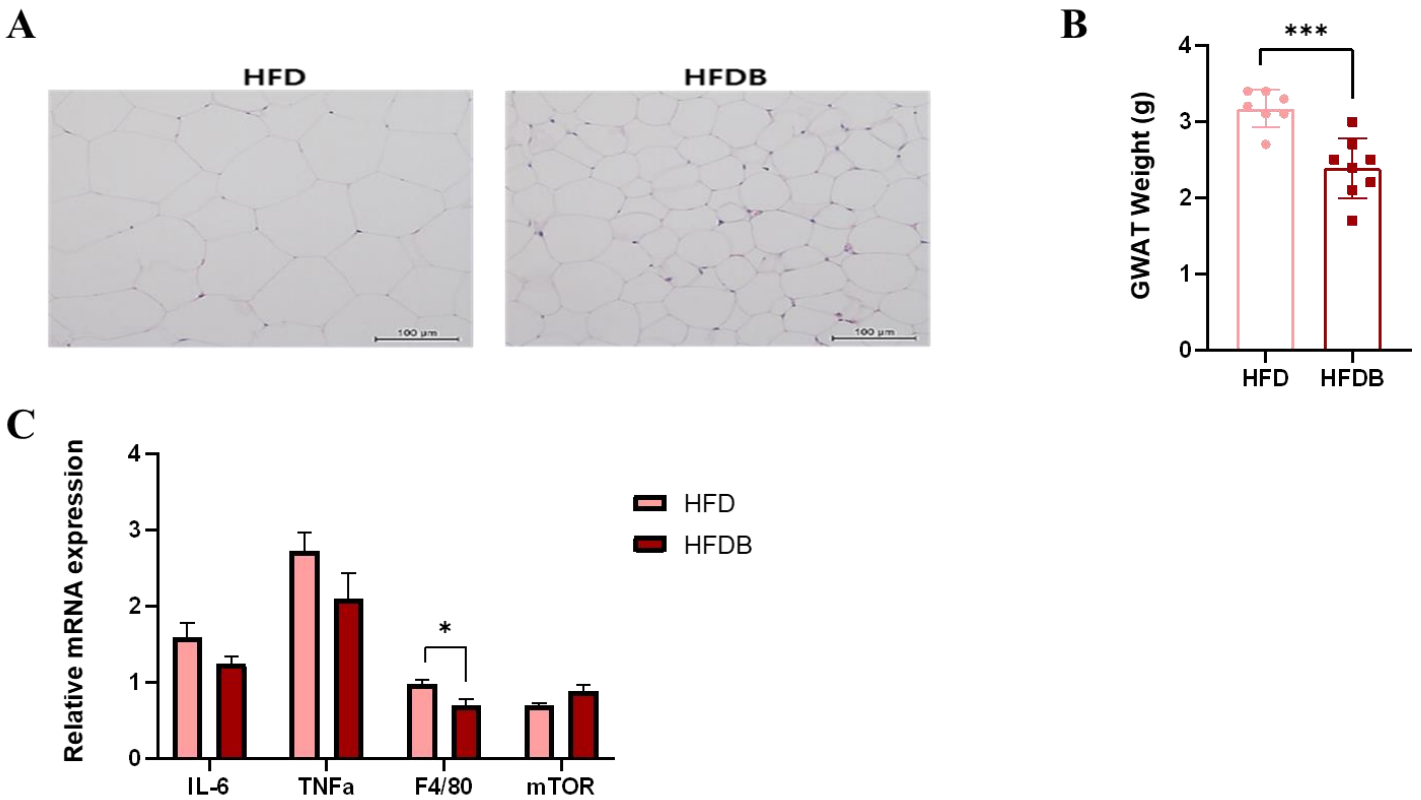
A
HFD
HFDB
100 μm
100 μm
B
***
GWAT Weight (g)
0
1
2
3
4
HFD
HFDB
C
Relative mRNA expression
0
1
2
3
4
*
IL-6
TNFa
F4/80
mTOR
HFD
HFDB

Figure 3. BV SNUG40005 reduced adipose tissue weight and inflammation in a DIO mouse model induced by high-fat diet.

At sacrifice, adipose tissue from mice was isolated and analyzed. (A) The gonadal adipose tissue was stained by H&E to determine the size of adipose cell. (B) The weight of the GAT was measured. Each value represents each mouse. (C) Pro-inflammatory cytokine IL-6, TNFa and inflammation indicator F4/80, mTOR are measured, represented by a bar plot. Statistical analysis was performed using a one-tailed unpaired t test based on 12 mice per group and error bars represent SEM. *, $P < 0.05$; **, $P < 0.01$; ***, $P < 0.001$.

3. Administration of BV SNUG40005 restore glucose intolerance and serum insulin level.

Glucose intolerance test was performed 16 weeks after administration to check glucose intolerance in BV-administered mice. Before the experiment, feed is starved for 16 hours to check for fasting blood glucose. Glucose was injected based on mouse weight, blood glucose level was measured at 6 time points. When GTT was performed, blood glucose peaked 30 minutes after glucose injected, and the peak value did not differ between the two groups. As blood glucose level decreased, the BV-administered group tended to decrease more than the PBS-treated group at 60 minutes, and significantly decreased at 90 and 120 minutes (Fig. 4A). In addition, to measure the insulin concentration in blood glucose, serum was isolated after obtaining blood through cardiac blood after sacrifice. Serum insulin levels were measured using a Mouse Insulin ELISA Kit (Crystal Chem). Serum insulin was compared between BV SNUG40005 and PBS groups, serum insulin level decreased in BV-administered mice (Fig. 4B). As a result, glucose tolerance was improved in mice administered BV SNUG40005, and that insulin level of serum was also reduced to confirm that hyperglycemia due to obesity was alleviated.

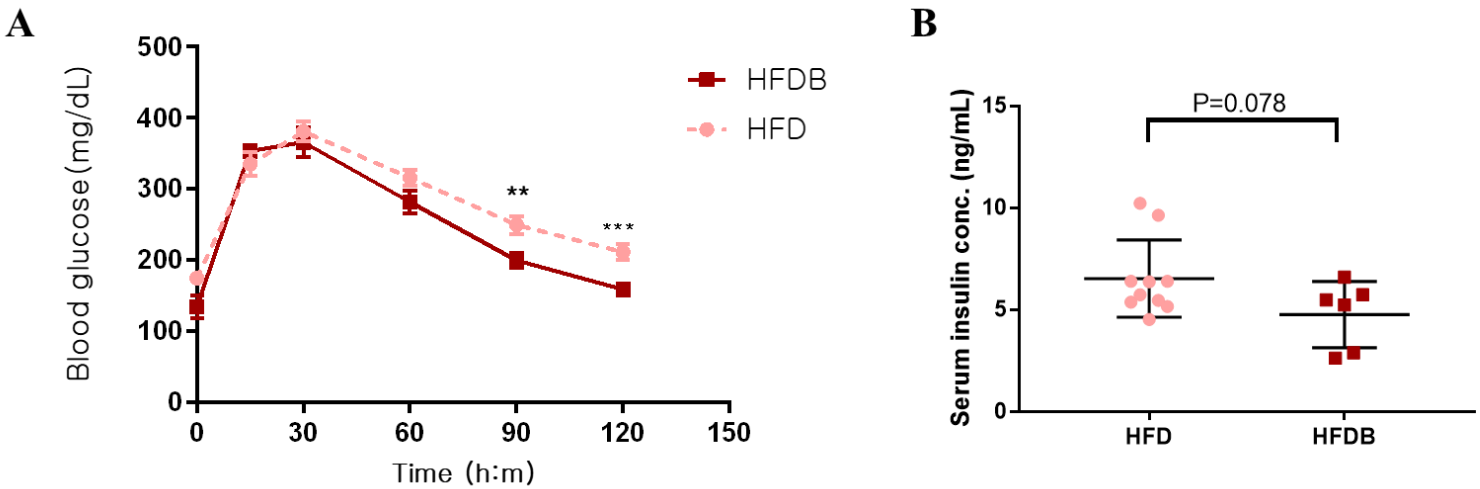

Figure 4. Administration of BV SNUG40005 restore glucose intolerance and insulin level in a serum of mice

(A) Blood glucose level was measured at 6 time points (15min, 30min, 60min, 90min, 120min). The value represents the mean value of the group. (B) Serum insulin levels were measured using a Mouse Insulin ELISA Kit (Crystal Chem). Each value represents each mouse. Statistical analysis was performed using a one-tailed unpaired t test of two groups and error bars represent SEM. *, $P < 0.05$; **, $P < 0.01$; ***, $P < 0.001$

4. BV SNUG40005 administration changed community structure of the fecal microbiota.

We next look at the effect of BV SNUG40005 on the composition of the intestinal microbiota. Stool samples were collected before and after antibiotic drinking water, after 5 days, 9 weeks, and 18 weeks. Fecal DNA was extracted, and microbiome structures were compared based on 16S rRNA gene. To compare the anti-obesity effects of BV SNUG40005 on a microbiome basis, the comparison with the ND and NDB groups was conducted together. First, the similarities of microbiota structures between groups were compared using Principal Coordinates Analysis (PCoA) Plot. In the ND group, when the BV SNUG40005 is administered, the structure is different compared to the control group, and the HFD group is also confirmed that the structure is changed when the BV SNUG40005 is administered (Fig. 5A). When comparing alpha diversity between groups at each time point, when treated with antibiotics, it decreases in all groups, after which it can be seen that there is some recovery. In the ND group, it can be seen that the alpha diversity is higher at all time points than the control group when BV SNUG40005 is administered. The alpha diversity of the HFD group is lower than that of the ND group at all timepoints, and it is slightly increased in BV SNUG40005 administration group (Fig. 5B). Based on this, in order to

confirm which specific bacterial strain difference, ND and HFD, and HFD and HFDB were compared and expressed as Gini index. In the ND group, the *g_Anaerotruncus*, *g_SMB53*, and *g_Akkermansia* strains were higher than the HFD group. When comparing the HFD group and the HFDB group, it can be seen that the strains *g_Streptococcus*, *g_Akkermansia*, and *g_Dialister* are high in the HFDB group (Fig. 5C). In order to compare the abundance of several major strains, relative abundance was compared by group based on the total amount of the strain. In the group fed HFD, we can see that *g_Akkermansia* and *g_Streptococcus* increase significantly when BV SNUG40005 is administered, and that *g_Oscillospira* decreases significantly (Fig. 5D). Through this, it was confirmed that the group of mice fed ND and the group fed HFD had an effect on the microbiota structure when BV SNUG40005 was administered, and several strains can be seen that there is a significant difference.

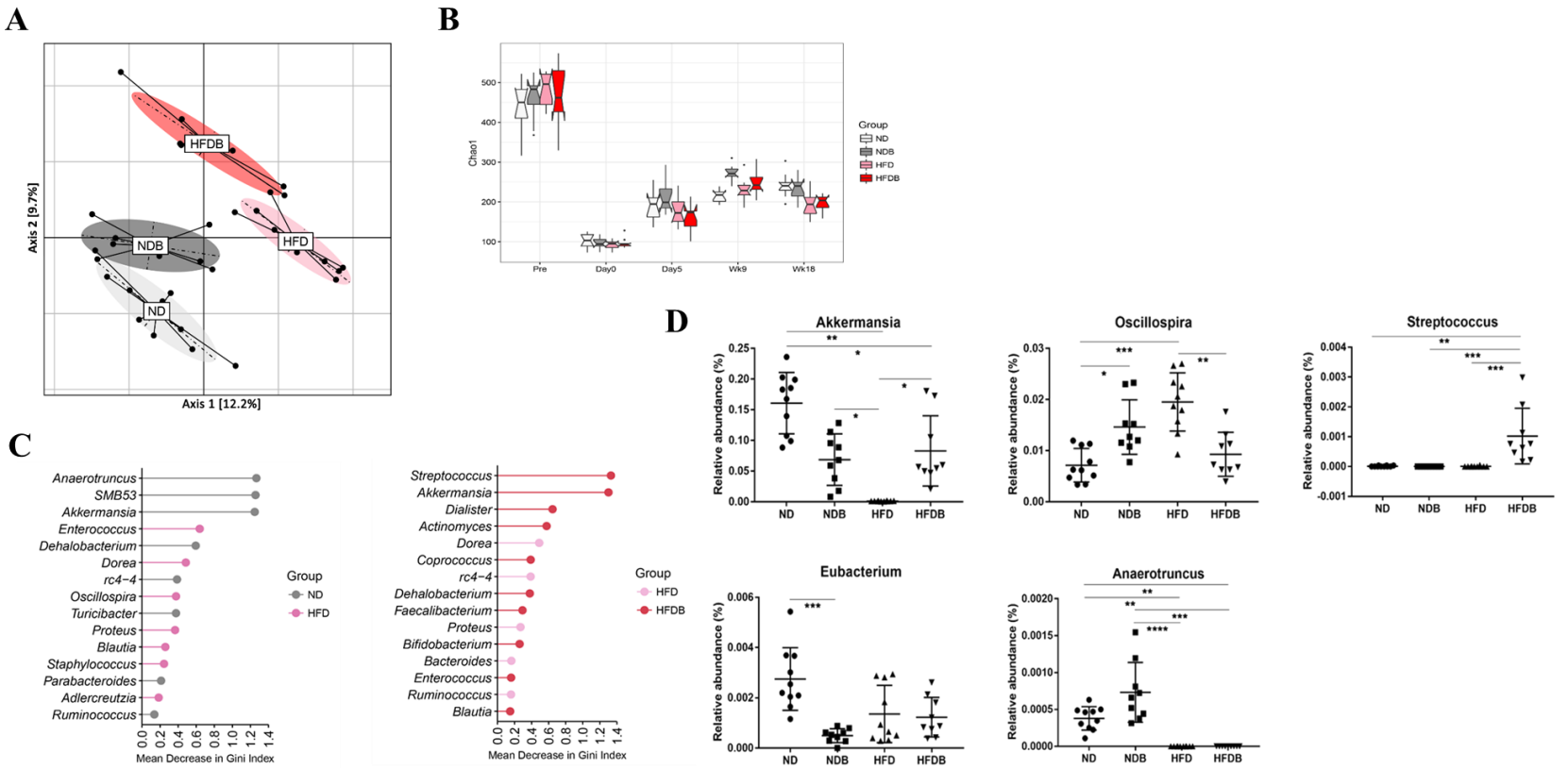
A
HFDB
NDB
HFD
ND
Axis 2 [9.7%]
Axis 1 [12.2%]
B
Chao1
Pre
Day0
Day5
Wk9
Wk18
Group
ND
NDB
HFD
HFDB
C
Anaerotruncus
SMB53
Akkermansia
Enterococcus
Dehalobacterium
Dorea
rc4−4
Oscillospira
Turicibacter
Proteus
Blautia
Staphylococcus
Parabacteroides
Adlercreutzia
Ruminococcus
Mean Decrease in Gini Index
Group
ND
HFD
Streptococcus
Akkermansia
Dialister
Actinomyces
Dorea
Coprococcus
rc4−4
Dehalobacterium
Faecalibacterium
Proteus
Bifidobacterium
Bacteroides
Enterococcus
Ruminococcus
Blautia
Mean Decrease in Gini Index
Group
HFD
HFDB
D
Akkermansia
Oscillospira
Streptococcus
Eubacterium
Anaerotruncus
Relative abundance (%)
ND
NDB
HFD
HFDB

Figure 5. Mouse fecal microbiota diversity and composition are changed by BV SNUG40005.

Microbiome analysis was processed with fecal samples at before and after antibiotic drinking water, after 5 days, 9 weeks, and 18 weeks. (A) PCoA plot of the fecal microbiota structure of 4 groups (ND, NDB, HFD, HFDB), measured by weighted UniFrac distance. (B) 4 groups of Chao1 diversity index represented at 5 time points. (C) Gini index of the genus level fecal microbiota in compare two groups, ND compared with HFD (left), HFD compared with HFDB (right). (D) Comparison of relative abundances of significantly different microbial taxa at the genus level. Each value represents each mouse fecal sample. Statistical analysis was performed using a one-tailed unpaired t test and error bars represent SEM. *, $P < 0.05$; **, $P < 0.01$; ***, $P < 0.001$; ****, $P < 0.0001$

5. BV SNUG40005 recovered mucus thickness in the group of mice fed HFD.

In mice administered BV SNUG40005, mucus layer thickness of colon tissue was measured to confirm the effect of improving intestinal environment. Colon tissue used Carnoy 's fixative to preserve the mucus layer after sacrifice. After fixing the colon tissue, paraffin embedding was performed and stored. After sectioning the slide glass with 4-um, tissues were stained using DAPI (blue), which stains the DNA of cells, and Wheat germ agglutinin (WGA-Alexa633, Green), which stains Mucus. The mucus layer was taken by confocal laser scanning microscopy and the thickness was measured by analytical software LAS X (Leica). In contrast, the green mucus layer, which was stained with green, remained thick in the BV-administered mouse, whereas it was reduced to half in the PBS-administered mouse (Fig. 6A). The measured values were taken of three positions in one sample, the average value was calculated by measuring three sites at each position, and the mucus layer thickness of the sample was calculated by calculating the average value of the three positions (Supplementary Table 1). In the mouse group administered BV SNUG40005, the mucus layer thickness was significantly higher (Fig. 6B). In relation to mucus layer and barrier function, LPS of serum was measured. Serum LPS was measured using

Mouse serum LPS KIT (CUSA BIO). Serum LPS level can also be found to be detected significantly less in the BV SNUG40005 group mice (Fig. 6C) Through this, the mucus layer is thickened and barrier function is improved in the BV-administered mice.

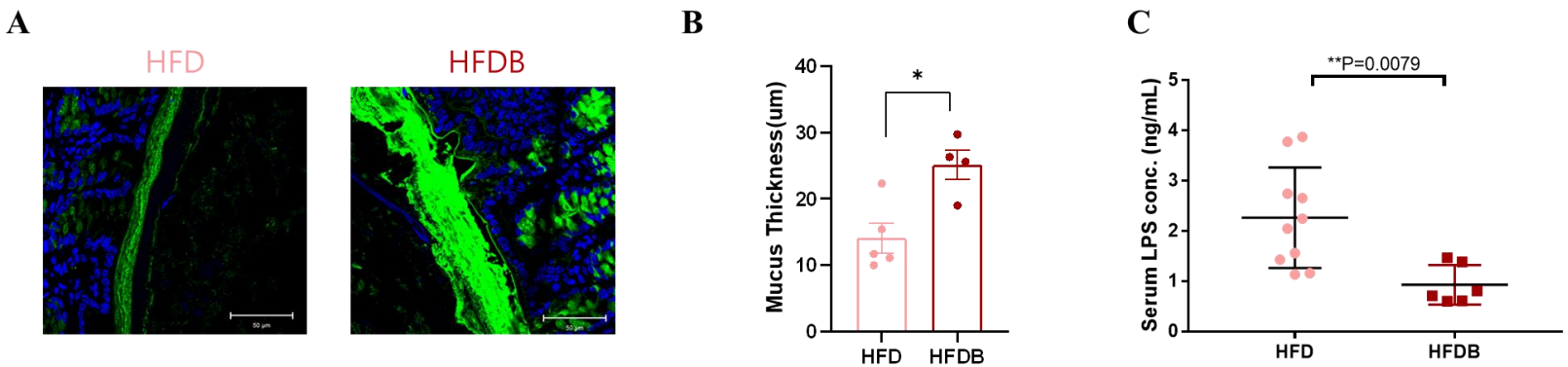

Figure 6. BV SNUG40005 recovered mucus layer thickness in a colon section and attenuated serum LPS level

Colon inner mucus layer thickness are measured. (A) Cross-sectioned colon tissues were stained using two distinct dyes. DAPI stains the DNA of cells (blue), Wheat germ agglutinin (WGA-Alexa633, green) stains mucus. (B) Measured mucus layer thickness represented by a bar plot. Each value represents each mouse mean of mucus layer thickness. (C) Serum LPS levels were measured using a Mouse LPS ELISA Kit (CUSA BIO). Each value represents each mouse. Statistical analysis was performed using a one-tailed unpaired t test based on independent experiments and error bars represent SEM. *, $P < 0.05$; **, $P < 0.01$.

6. Administration of BV SNUG40005 restore gene expression of mucus layer and tight junction related genes in colon.

In order to confirm the mucus layer recovery and barrier function improvement by BV SNUG40005, gene expression of mucus layer related gene and barrier function related gene in colon tissue was confirmed at RNA-level by real time PCR. The gene associated with mucus, the transmembrane glycoprotein Mucin 1, 13 (*Muc1*, *Muc13*), oligomeric mucus gel-forming Mucin 2 (*Muc2*), anti-adhesive roles in the body, such as in lubricating the reproductive lining Mucin 4 (*Muc4*), mucus secretion Kruppel-like factor 4 (*KLF4*), mucus production regulatory factor Interferon regulatory factor 4 (*IRF4*) are confirmed. *Muc1*, *Muc2*, *Muc4*, *Muc13*, *Klf4*, and *Irf4* all mucus related gene expressions were significantly increased in BV-administered mice compared to PBS- administered mice (Fig. 7A). The gene associated with tight junction, the peripheral membrane protein Zonula occludens-1 (*ZO-1*), integral plasma-membrane protein Occludin (*Occlu*), Claudin (*Clau*) are confirmed. The gene associated with bacteria invasion into epithelial, Regenerating islet-derived protein 3 gamma (*Reg3g*) via stimulation of toll-like receptors (TLRs) by pathogen-associated molecular patterns (PAMPs), barrier protective cytokine interleukin-22 (*IL-22*), stimulated bacteria invasion interleukin-23 (*IL-23*) and interleukin-25 (*IL-25*) are confirmed. Of the tight junction related genes,

only *Zo-1* was elevated in the BV SNUG40005 administration group (Fig. 7B). Among genes related to barrier infiltration, only *IL-23* was significantly reduced (Fig. 7B). Through this, mucus layer recovery effect and barrier function improvement effect can be confirmed in BV-administered mice.

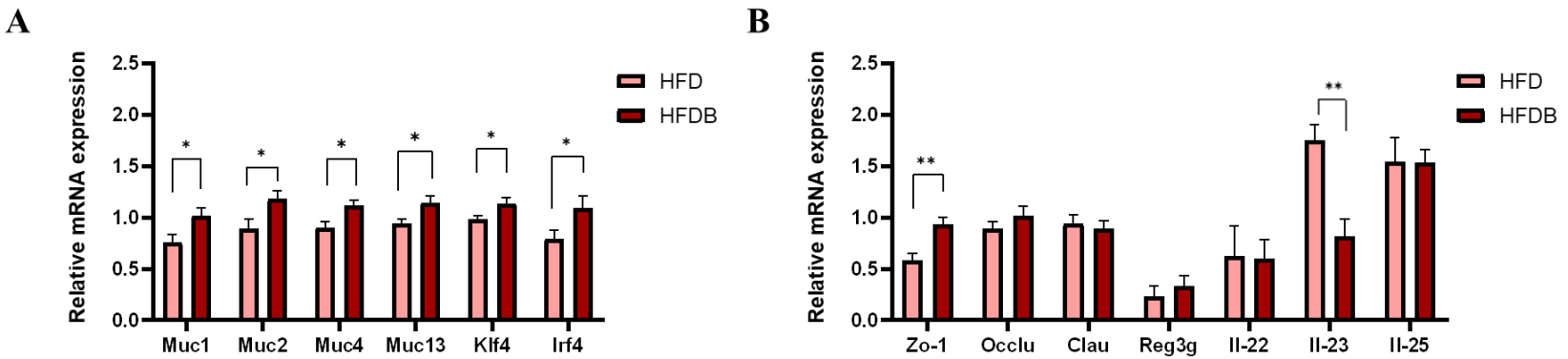

Figure 7. BV SNUG40005 restore gene expression of mucus layer and tight junction related genes in colon of DIO mice.

Colon was collected and measured mucus-related genes, tight junction related genes expression by real time PCR. (A) Mucus layer-related genes (*Muc1, Muc2, Muc4, Muc13, Klf4, Irf4*) relative gene expression compared HFD with HFDB group. (B) Tight junction related genes (*Zo-1*, Occludin (*Occlu*), Claudin (*Clau*), *Reg3g, IL-22, IL-23, IL25*) relative gene expression compared HFD with HFDB group. Data shown as bar plot graph. Statistical analysis was performed using a one-tailed unpaired t test of 12 mice per group and error bars represent SEM. *, $P < 0.05$; **, $P < 0.01$; ***, $P < 0.001$.

7. BV SNUG40005 increases gene expression associated with mucus layer and tight junction *in vitro.*

To verify mucus layer recovery and barrier function improvement by BV SNUG40005 *in vitro*, we treated BV SNUG40005 in human colonic epithelial cell line, and confirmed mucus layer-related gene expression and tight-junction-related gene expression at RNA-level. Mucus layer-related gene expression *(Muc2, Muc13, Klf4*) used goblet-like cell line LS174T cell, tight-junction-related gene expression (*Zo-1, Occludin*) was colon epithelial cell line Caco-2 cell Was used. Both cell lines were seeded at $1x10^6$ cells/well on a 6 well plate, and 24 hours after seeding, PBS (control -CON), Pasteurization BV SNUG40005 (PAS), BV SNUG40005 $1x10^7$ bacteria/well (BV 10^7), BV SNUG40005 $1x10^8$ bacteria/well (BV 10^8) were treated, the experiment was carried out under four conditions. Pasteurization BV SNUG40005 was used after pasteurize at 65 ° C for 30 minutes, and used to determine whether the effect of bacteria was associated with living cell activity. In addition, two concentrations of bacteria were treated to determine the dose dependency of the bacteria effect. In the case of *Muc2*, gene expression was significantly increased in BV 10^8 compared to the control group, but no increase in gene expression was observed in the Pas and BV 10^7 groups (Fig. 8A). *Muc13* also showed a similar pattern to *Muc2*, and gene expression increased only under the conditions of BV 10^8 (Fig. 8B).

Klf4 did not show any changes in gene expression under all conditions (Fig. 8C). In the case of *Zo-1*, gene expression was significantly increased in BV 10^8 compared to the control group, but no increase in gene expression was observed in the Pas and BV 10^7 groups (Fig. 8D). *Occludin* also showed a similar pattern to *Zo-1*, there was a tendency to increase gene expression in BV 10^8 condition compared to the control group, but not significant (Fig. 8E). Through this, we could verify mucus layer recovery effect and barrier function improvement effect by BV SNUG40005 in human cell line, and this confirmed that it appeared in the concentration more than BV 10^8. These experimental results can be seen that the appearance similar to the mouse experiment.

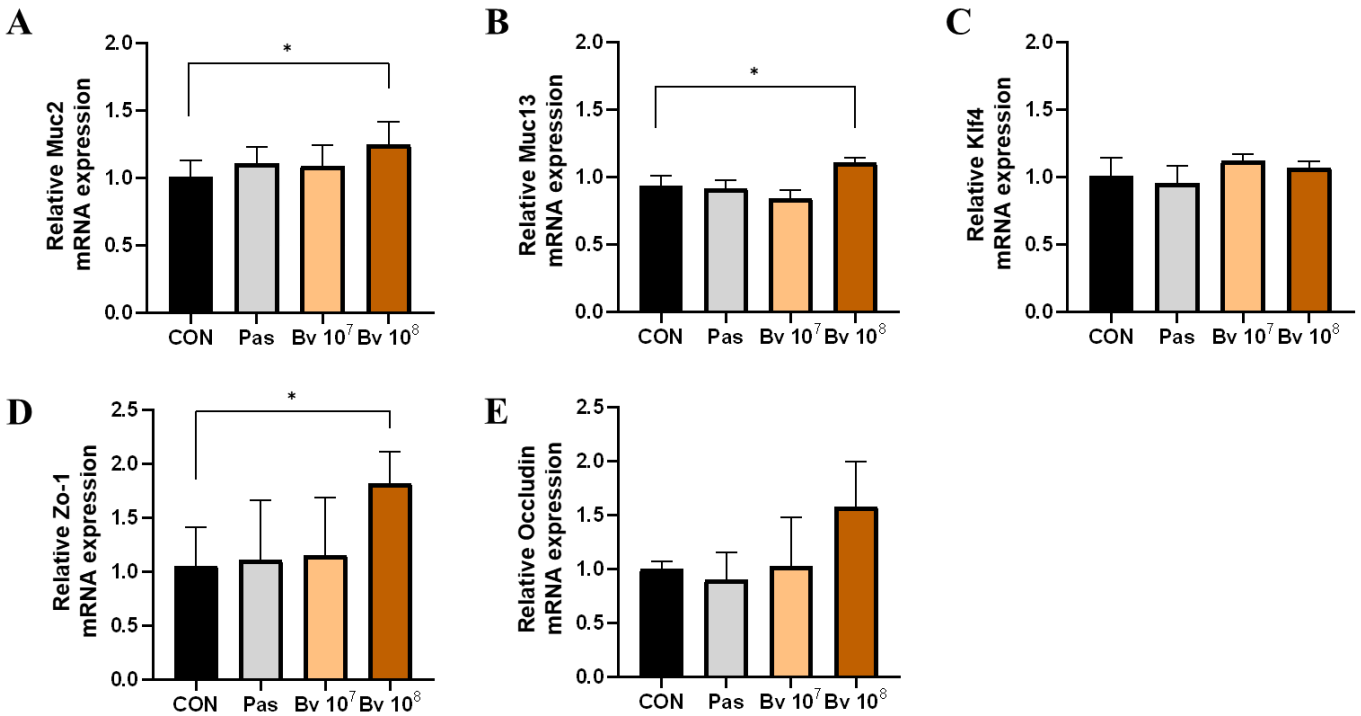
A
Relative Muc2 mRNA expression
2.0
1.5
1.0
0.5
0.0
*
CON
Pas
Bv 10^7
Bv 10^8
B
Relative Muc13 mRNA expression
2.0
1.5
1.0
0.5
0.0
*
CON
Pas
Bv 10^7
Bv 10^8
C
Relative Klf4 mRNA expression
2.0
1.5
1.0
0.5
0.0
CON
Pas
Bv 10^7
Bv 10^8
D
Relative Zo-1 mRNA expression
2.5
2.0
1.5
1.0
0.5
0.0
*
CON
Pas
Bv 10^7
Bv 10^8
E
Relative Occludin mRNA expression
2.5
2.0
1.5
1.0
0.5
0.0
CON
Pas
Bv 10^7
Bv 10^8

Figure 8. BV SNUG40005 increase gene expression associated with mucus layer and tight junction in human colon epithelial cell line Caco-2 and LS174T.

Confirm the effect of improving the barrier function, an *in-vitro* experiment was performed to treat BV in human cell lines. The treatment was performed under three conditions: pasteurized BV SNUG40005 (Pas), BV SNUG40005 $1x10^7$ bacteria/well (BV 10^7), BV SNUG40005 $1x10^8$ bacteria/well (BV 10^8), and the gene expression was confirmed by real-time PCR. Gene expression represented (A) *Muc2*, (B) *Muc13*, (C) *Klf4* using LS174T, (D) *Zo-1*, (E) *Occludin* using Caco-2. Data shown as bar plot graph (n=4, respectively), statistical analysis was performed using a one-tailed unpaired t test and error bars represent SEM. *, $P < 0.05$; **, $P < 0.01$; ***, $P < 0.001$.

8. BV SNUG40005 recover gene expression associated with tight junction in an oxidative stress model induced by ASA in vitro.

Thus far, it can be seen that the improvement of barrier function of BV SNUG40005 is most prominent in *Zo-1* gene expression of tight junction. Therefore, to apply the barrier function improvement by BV SNUG40005 to *Zo-1* in the obesity model, the acetylsalicylic acid (ASA) stress model was used. Obesity-induced mice have stress on colon epithelial cells. ASA is known to give oxidative stress in the Caco-2 cell line, in particular it is known to have a critical effect on the *Zo-1* gene expression. In order to confirm the recovery effect by BV SNUG40005 in an oxidative stress, ASA was treated in Caco-2 cell line to induce oxidative stress, followed by BV SNUG40005 treatment, and the recovery effect was confirmed by RNA gene expression. n the previous experiment, the effect of BV SNUG40005 was confirmed at $1x10^8$ bacteria / well, so all were treated with $1x10^8$ and compared with Pasteurization BV SNUG40005 and Live BV SNUG40005 to confirm the living bacteria activity. In the case of *Zo-1* gene, gene expression was significantly decreased when ASA was treated, but no stress effect was observed in *Occludin* or *Claudin* (Fig. 9A to C). When treated with BV SNUG40005, *Zo-1* was found to recover significantly from the ASA treat group, in the Pasteurization BV SNUG40005 group, there was a tendency of recovery but no significance (Fig. 9A). *Occludin* or *Claudin*

showed no stress effect of ASA and no increase effect of BV SNUG40005 (Fig. 9B and C). This suggests that BV SNUG40005 exhibits a significant recovery effect on *Zo-1* under stress of colon epithelial, and the same pattern as in mouse experiments.

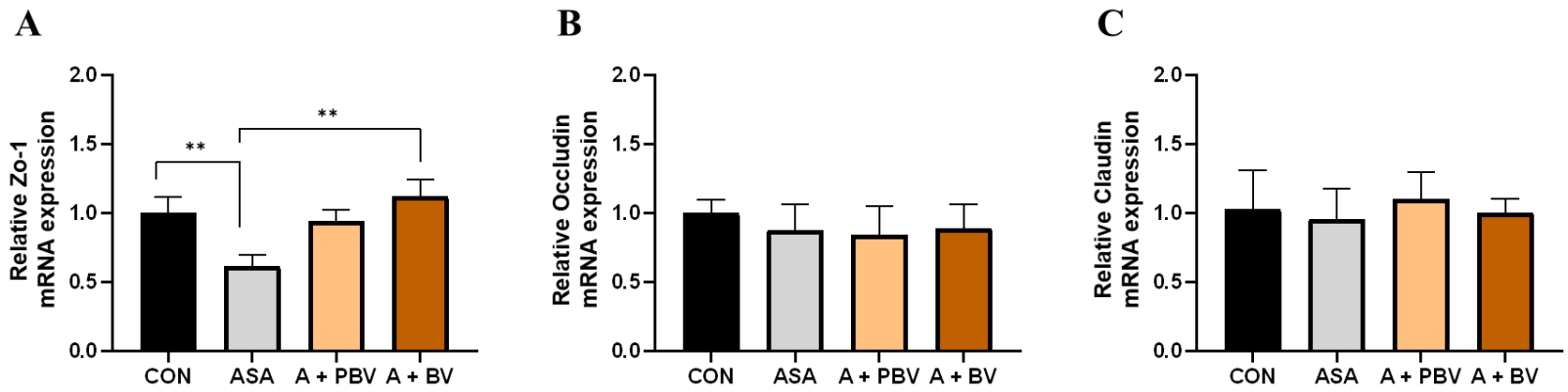

Figure 9. BV SNUG40005 recover gene expression associated with tight junction in an oxidative stress model induced by ASA in human colon epithelial cell line Caco-2.

Confirm the effect of recover the barrier function in epithelial stress, an *in-vitro* experiment was performed to treat BV SNUG40005 in Caco-2 cell lines. The treatment was performed under three conditions: stressed by acetylsalicylic acid treated (ASA), ASA treated with pasteurized BV SNUG40005 (A+PBV), ASA treated with BV SNUG40005 $1x10^8$ bacteria/well (A+BV), and the gene expression was confirmed by real-time PCR. Gene expression represented (A) *Zo-1*, (B) *Occludin*, (C) *Claudin* using Caco-2. Data shown as bar plot graph (n=4, respectively), statistical analysis was performed using a one-tailed unpaired t test and error bars represent SEM. *, $P < 0.05$; **, $P < 0.01$; ***, $P < 0.001$.

IV. Discussion

In this study, we identified the anti-obesity effect of isolated BV SNUG40005 in a high fat diet induced obesity mouse model. We validated the recovery of mucus layer and barrier function as one of the major mechanisms of anti-obesity effect by BV SNUG40005. In addition, using two human colonic epithelial cell lines, we found that BV SNUG40005 directly affects gene expression in epithelial cell lines. Also, we revealed that the administration of BV SNUG40005 affected the microbiota structure, and several strains significantly recovered by BV SNUG40005 treatment during HFD-induced dysbiosis.

The genus *Bacteroides* belongs to the *Bacteroidetes* family, and is known as a major gut microbiota in adults along with *Firmicutes*.[21-23] In the case of the B / F ratio, which represents the ratio of *Bacteroidetes* and *Firmicutes*, many clinical studies and animal studies have reported negative correlations in diseases such as obesity, diabetes, arteriosclerosis, and IBD.[23-25] In addition, many studies reported *Bacteroides* has an efficient polymer-degrading activity on various food-derived dietary fiber and polysaccharides[26], produce a variety of metabolites such as short chain fatty acids[27] and contributes to colonization and stabilization of commensal gut microbiota including probiotic strains.[28]

In this study, it was confirmed that the BV SNUG40005 administered group was effective in alleviating obesity and changing the structure of intestinal microorganisms. Even with normal diet, body weight was slightly reduced, but the effect was high on high fat diet (Supplemental Fig. 1A-D). Since the administration of BV SNUG40005 also affected the weight of the normal diet group, we measured food intake and calorie intake (Supplemental Fig. 3A-B). As a result, no significant difference was observed in food intake and in calorie intake both ND and HFD groups. Therefore, weight loss in the ND group may have other effects induced by altered microbiota structure or microbe-host interaction, and further study is needed. When obesity is induced, adipocytes become larger (hyperplasia), and once grown, adipocytes are not easily got smaller.[29] In this study, we collected the gonadal adipose tissue and measured the changes in adipocytes size. When BV SNUG40005 was administered, the size of adipocytes was remarkably reduced and the inflammatory response in adipose tissue was also decreased, indicating the preventive effect of BV SNUG40005 on fat accumulation during obesity.

Hyperglycemia is a major complication in obese patients.[30, 31] Most diet-induced obese patients easy to be exposed to complications such as type 2 diabetes and hyperglycemia.[32] In this study, significant improvement of glucose intolerance and insulin sensitivity by BV

SNUG40005 administration were confirmed by IPGTT and insulin measurement. In previous studies, *Bacteroides* strains were reported to sustain and modulate the intestinal microbiota. For example, the ability of *B. fragilis* to tolerate and use oxygen, they use P_{O2} for their growth, and by regulating the concentration of oxygen in the intestinal environment, it affects the intestinal microbiota.[33] In addition, *Bacteroides* suggests a tremendous capacity to use a wide range of dietary polysaccharides. For instance, *B. thetaiotaomicron* has Sus C proteins, so succinate can be used as an energy source. Also, *B. fragilis* has Sus C-like component may be a conserved component of multifunctional outer membrane proteins.[34] Therefore, *Bacteroides* use various polysaccharides and produce various by- products or metabolites that affect the intestinal microbiota.[35] In this study, g_*Streptococcus*, g_*Akkermansia*, and g_*Dialister* were changed significantly, when BV SNUG40005 was administered compared with HFD control group. Among them, *Akkermansia* strains are widely known as beneficial strains to host, and there are reports of weight loss effects.[36] In the clinical study of *Akkermansia muciniphila*, shows a high abundance in healthy-normal weight people.[37] In addition, negative correlations of *Akkermansia muciniphila* with fasting plasma glucose, plasma triglycerides and body fat distribution have been reported.[38] Therefore, the correlation between BV SNUG40005

(*Bacteroides vulgatus*) and *Akkermansia* seems to be important and further study is needed.

Bacteroides strains are also related with the inflammatory response and the immune system. In the case of capsular polysaccharide A (PSA) produced by *Bacteroides fragilis* promotes the release of an anti-inflammatory cytokine IL-10 from host immune cells including Tregs.[15] In addition, *Bacteroides thetaiotaomicron* were reported to show improving barrier function through promoting host IL-10 production, and antigen produced by *Bacteroides thetaiotaomicron* regulates the T cell response of the host has been reported.[39] In rabbits, the combination of *B. fragilis* and *Bacillus subtilis* consistently promoted GALT (gut-associated lymphoid tissues) development and led to development of the pre-immune antibody repertoire.[40] In this study, in order to verify the anti-inflammatory effect of the BV SNUG40005, various *Bacteroides* strains were treated on the human monocyte cell line THP-1 cell. Supernatants were collected during the differentiation of macrophage and the ratio of *IL-10* and *TNF-a* was compared by ELISA. As a result, among the various *Bacteroides* strains, it showed the highest IL-10/TNF -a ratio in isolated BV SNUG40005 and was selected as the experimental strain. (Supplemental Fig. 2). In addition, the suppression of F4/80 gene expression could confirm the effect of BV SNUG40005 on the macrophage innate immune response.[41] Through this, BV

SNUG40005 also affects the host's immune system, and further study related with host immune system and BV SNUG40005 is required.

In obese patients, the barrier function is reduced and the mucus layer is relatively thin.[42] Therefore, leaky gut syndrome is more likely to develop. When leaky gut syndrome is induced, intestinal pathogens, PAMPs, LPS, and other bad substances infiltrate the body indiscriminately, causing various intestinal diseases or host inflammatory reactions that adversely affect the immune system.[43] Therefore, improving leaky gut syndrome in obese patients is an important issue. In this study, both mucus layer and increased intestinal permeability due to obesity were significantly improved when BV SNUG40005 was treated in both *in vivo* and *in vitro*.

In order to confirm improvement in the gut environment by BV SNUG40005, the colon was collected to identify mucus-related gene, tight junction related gene and barrier dysfunction related gene expression *in vivo.* Mucin 1, 4, 13 (*Muc1, Muc4, Muc13*) is a transmembrane glycoprotein and forms mucins between cells.[44-46] Mucin 2 (*Muc2*) is the most important protein for the production of mucus layer and oligomeric mucus gel-forming protein that secretes mucus from epithelial cells.[47, 48] *KLF4* is known to stimulate on goblet cells and promote mucus secretion.[49] *IRF4* has also been reported to be involved in the production of mucus.[50] Therefore,

mucus layer related genes plays an important role in gut barrier function, and restoring, it is essential to prevent leaky gut syndrome due to obesity. In this experiment, it was confirmed that the expression of all genes mentioned in the BV SNUG40005-administered group increased significantly compared to the control group. Thus, it can be seen that BV SNUG40005 restores mucus layer destruction due to obesity. *Zo-1, Occludin* and *Claudin* are major proteins that make up tight junctions.[51-53] Therefore, decreased expression of these genes increases cell permeability, which can lead to leaky gut syndrome due to the indiscriminate influx of intestinal impurities. In this experiment, BV SNUG40005 was found to significantly increase *Zo-1* among the tight junction proteins. Therefore, the effect of BV SNUG40005 can be seen to increase the tight junction as well as the mucus layer, it can be seen that can prevent the leaky gut syndrome. In addition, *Reg3g*, *IL-22*, *IL23*, and *IL-25* were confirmed to identify bacteria invasion into epithelial.[54-56] These proteins are related to barrier protection to confirm invasion from the outside in epithelial cells. In this experiment, *IL-23* was significantly increased in BV SNUG40005 administered group. IL-23, a cytokine stimulated when cell damaged in colon epithelial, has been reported to help repair damaged cells.[57] Therefore, it can be seen that BV SNUG40005 plays an important role in improving intestinal environmental function by increasing expression of various

barrier related genes expression *in vivo*.

In vitro experiments showed that the effect of the BV SNUG40005 in the pasteurization group was not effective. Through this, it can be seen that the effect of improving the intestinal environment of BV SNUG40005 is effective when they are alive, so metabolism byproducts or metabolites from BV SNUG40005 seem to play an important role. However, further study is needed to determine whether the effect is altered intestinal microbiota or bacterial metabolites.

To show the intestinal environment stressed by obesity, we used a model that increased permeability by giving oxidative stress to Caco-2 cells. Permeability was damaged using acetylsalicylic acid (ASA). ASA has been reported to reduce the gene expression of *Zo-1*, a tight junction protein, by giving oxidative stress to Caco-2 cells.[58] Therefore, in this study, we treat ASA in Caco-2 cells to induce oxidative stress, increase permeability, and confirm the recovery effect of BV SNUG40005. In this experiment, it was also confirmed that pasteurization BV SNUG40005 had a lower effect than live BV SNUG40005 on recover expression of Zo-1 protein. In the case of live BV SNUG40005, *Zo-1* gene expression was restored to the control level, indicating an improvement in permeability. Therefore, we can expect direct permeability improvement effect by BV SNUG40005 metabolites or byproduct on colon epithelial cells that got damaged due to obesity.

In summary, this study successfully confirmed the anti-obesity effect of BV SNUG40005 through the improvement of intestinal environment and the change of intestinal microbiota. BV SNUG40005 altered gut microbiota in both HFD and ND groups and increased abundance of beneficial microorganisms in HFD group. In addition, increased expression of mucus layer and tight junction related genes was demonstrated *in vivo* and *in vitro*. However, the limitation of this study was not able to elucidate the detailed mechanism of intestinal environment improvement effect by BV SNUG40005. Therefore, further studies on the impact on metabolism or microbiota environment by BV SNUG40005 are needed. Accordingly, this study can suggest a possibility for the treatment of BV SNUG40005 in obesity.

References

1. Stefan, N., F. Schick, and H.U. Haring, *Causes, Characteristics, and Consequences of Metabolically Unhealthy Normal Weight in Humans.* Cell Metab, 2017. **26**(2): p. 292-300.
2. Hensrud, D.D. and S. Klein, *Extreme Obesity: A New Medical Crisis in the United States.* Mayo Clinic Proceedings, 2006. **81**(10, Supplement): p. S5-S10.
3. Re, R.N., *Obesity-related hypertension.* The Ochsner journal, 2009. **9**(3): p. 133-136.
4. Basen-Engquist, K. and M. Chang, *Obesity and cancer risk: recent review and evidence.* Current oncology reports, 2011. **13**(1): p. 71-76.
5. de Heredia, F.P., S. Gómez-Martínez, and A. Marcos, *Obesity, inflammation and the immune system.* Proceedings of the Nutrition Society, 2012. **71**(2): p. 332-338.
6. Everard, A. and P.D. Cani, *Diabetes, obesity and gut microbiota.* Best Practice & Research Clinical Gastroenterology, 2013. **27**(1): p. 73-83.
7. Sartor, R.B. and G.D. Wu, *Roles for Intestinal Bacteria, Viruses, and Fungi in Pathogenesis of Inflammatory Bowel Diseases and Therapeutic Approaches.* Gastroenterology, 2017. **152**(2): p. 327-339.e4.
8. Agustí, A., et al., *Interplay Between the Gut-Brain Axis, Obesity and Cognitive Function.* Frontiers in neuroscience, 2018. **12**: p. 155-155.
9. Cerf-Bensussan, N. and V. Gaboriau-Routhiau, *The immune system and the gut microbiota: friends or foes?* Nature Reviews Immunology, 2010. **10**(10): p. 735-744.
10. Ellulu, M.S., et al., *Obesity and inflammation: the linking mechanism and the complications.* Archives of medical science : AMS, 2017. **13**(4): p. 851-863.
11. Castaner, O., et al., *The Gut Microbiome Profile in Obesity: A Systematic Review.* Int J Endocrinol, 2018. **2018**: p. 4095789.
12. Koliada, A., et al., *Association between body mass index and Firmicutes/Bacteroidetes ratio in an adult Ukrainian population.* BMC Microbiology, 2017. **17**(1): p. 120.
13. Méndez-Salazar, E.O., et al., *Altered Gut Microbiota and Compositional Changes in Firmicutes and Proteobacteria in Mexican Undernourished and Obese Children.* Frontiers in Microbiology, 2018. **9**(2494).
14. Mazmanian, S.K., et al., *An Immunomodulatory Molecule of Symbiotic Bacteria Directs Maturation of the Host Immune System.* Cell, 2005. **122**(1): p. 107-118.
15. Troy, E.B. and D.L. Kasper, *Beneficial effects of Bacteroides fragilis polysaccharides on the immune system.* Frontiers in bioscience (Landmark edition), 2010. **15**: p. 25-34.
16. Azad, M.A.K., et al., *Probiotic Species in the Modulation of Gut Microbiota: An Overview.* Biomed Res Int, 2018. **2018**: p. 9478630.
17. Weng, M. and W.A. Walker, *Bacterial colonization, probiotics, and clinical disease.* The Journal of Pediatrics, 2006. **149**(5, Supplement): p. S107-S114.
18. Johansson, M.E. and G.C. Hansson, *Preservation of mucus in histological sections, immunostaining of mucins in fixed tissue, and localization of bacteria with FISH.* Methods Mol Biol, 2012. **842**: p. 229-35.
19. Andrikopoulos, S., et al., *Evaluating the glucose tolerance test in mice.* Am J Physiol Endocrinol Metab, 2008. **295**(6): p. E1323-32.
20. Macierzanka, A., et al., *Transport of Particles in Intestinal Mucus under*

Simulated Infant and Adult Physiological Conditions: Impact of Mucus Structure and Extracellular DNA. PLOS ONE, 2014. **9**(4): p. e95274.
21. Gibiino, G., et al., *Exploring Bacteroidetes: Metabolic key points and immunological tricks of our gut commensals.* Digestive and Liver Disease, 2018. **50**(7): p. 635-639.
22. Yoshida, N., et al., *Bacteroides vulgatus and Bacteroides dorei Reduce Gut Microbial Lipopolysaccharide Production and Inhibit Atherosclerosis.* Circulation, 2018. **138**(22): p. 2486-2498.
23. Gill, S.R., et al., *Metagenomic Analysis of the Human Distal Gut Microbiome.* Science, 2006. **312**(5778): p. 1355.
24. Zhou, Y. and F. Zhi, *Lower Level of Bacteroides in the Gut Microbiota Is Associated with Inflammatory Bowel Disease: A Meta-Analysis.* BioMed Research International, 2016. **2016**: p. 9.
25. Ley, R.E., et al., *Obesity alters gut microbial ecology.* Proceedings of the National Academy of Sciences of the United States of America, 2005. **102**(31): p. 11070.
26. Wexler, A.G. and A.L. Goodman, *An insider's perspective: Bacteroides as a window into the microbiome.* Nature Microbiology, 2017. **2**(5): p. 17026.
27. Rios-Covian, D., et al., *Shaping the Metabolism of Intestinal Bacteroides Population through Diet to Improve Human Health.* Frontiers in Microbiology, 2017. **8**(376).
28. Sonnenburg, J.L., L.T. Angenent, and J.I. Gordon, *Getting a grip on things: how do communities of bacterial symbionts become established in our intestine?* Nature Immunology, 2004. **5**(6): p. 569-573.
29. de Ferranti, S. and D. Mozaffarian, *The Perfect Storm: Obesity, Adipocyte Dysfunction, and Metabolic Consequences.* Clinical Chemistry, 2008. **54**(6): p. 945.
30. Martyn, J A.J.M.D.F.R.C.A.F.C.C.M., M.M.D.P.D. Kaneki, and S.M.D.P.D. Yasuhara, *Obesity-induced Insulin Resistance and Hyperglycemia: Etiologic Factors and Molecular Mechanisms.* Anesthesiology: The Journal of the American Society of Anesthesiologists, 2008. **109**(1): p. 137-148.
31. Thaiss, C.A., et al., *Hyperglycemia drives intestinal barrier dysfunction and risk for enteric infection.* Science, 2018. **359**(6382): p. 1376.
32. Martyn, J.A.J., M. Kaneki, and S. Yasuhara, *Obesity-induced insulin resistance and hyperglycemia: etiologic factors and molecular mechanisms.* Anesthesiology, 2008. **109**(1): p. 137-148.
33. Baughn, A.D. and M.H. Malamy, *The strict anaerobe Bacteroides fragilis grows in and benefits from nanomolar concentrations of oxygen.* Nature, 2004. **427**(6973): p. 441-444.
34. Xu, J., et al., *A Genomic View of the Human-Bacteroides thetaiotaomicron Symbiosis.* Science, 2003. **299**(5615): p. 2074.
35. Xu, J. and J.I. Gordon, *Honor thy symbionts.* Proceedings of the National Academy of Sciences, 2003. **100**(18): p. 10452.
36. Everard, A., et al., *Cross-talk between Akkermansia muciniphila and intestinal epithelium controls diet-induced obesity.* Proceedings of the National Academy of Sciences, 2013. **110**(22): p. 9066.
37. Depommier, C., et al., *Supplementation with Akkermansia muciniphila in overweight and obese human volunteers: a proof-of-concept exploratory study.* Nature Medicine, 2019. **25**(7): p. 1096-1103.
38. Dao, M.C., et al., *Akkermansia muciniphila and improved metabolic health during a dietary intervention in obesity: relationship with gut microbiome richness and ecology.* Gut, 2016. **65**(3): p.

426.
39. Wegorzewska, M.M., et al., *Diet modulates colonic T cell responses by regulating the expression of a Bacteroides thetaiotaomicron antigen.* Science Immunology, 2019. **4**(32): p. eaau9079.
40. Rhee, K.-J., et al., *Role of Commensal Bacteria in Development of Gut-Associated Lymphoid Tissues and Preimmune Antibody Repertoire.* The Journal of Immunology, 2004. **172**(2): p. 1118.
41. Lin, H.-H., et al., *The macrophage F4/80 receptor is required for the induction of antigen-specific efferent regulatory T cells in peripheral tolerance.* The Journal of experimental medicine, 2005. **201**(10): p. 1615-1625.
42. Hofer, U., *A mucus colonizer manages host metabolism.* Nature Reviews Microbiology, 2013. **11**: p. 430.
43. Agustí, A., et al., *Interplay Between the Gut-Brain Axis, Obesity and Cognitive Function.* Frontiers in Neuroscience, 2018. **12**(155).
44. Nath, S. and P. Mukherjee, *MUC1: a multifaceted oncoprotein with a key role in cancer progression.* Trends in molecular medicine, 2014. **20**(6): p. 332-342.
45. Carraway, K.L., et al., *Muc4/MUC4 functions and regulation in cancer.* Future oncology (London, England), 2009. **5**(10): p. 1631-1640.
46. Sheng, Y.H., et al., *MUC1 and MUC13 differentially regulate epithelial inflammation in response to inflammatory and infectious stimuli.* Mucosal Immunology, 2013. **6**(3): p. 557-568.
47. Johansson, M.E.V., J.M.H. Larsson, and G.C. Hansson, *The two mucus layers of colon are organized by the MUC2 mucin, whereas the outer layer is a legislator of host–microbial interactions.* Proceedings of the National Academy of Sciences, 2011. **108**(Supplement 1): p. 4659-4665.
48. Cobo, E.R., et al., *Colonic MUC2 mucin regulates the expression and antimicrobial activity of β-defensin 2.* Mucosal Immunology, 2015. **8**(6): p. 1360-1372.
49. Katz, J.P., et al., *The zinc-finger transcription factor Klf4 is required for terminal differentiation of goblet cells in the colon.* Development, 2002. **129**(11): p. 2619.
50. Williams, J.W., et al., *Transcription factor IRF4 drives dendritic cells to promote Th2 differentiation.* Nature communications, 2013. **4**: p. 2990-2990.
51. Van Itallie, C.M., et al., *ZO-1 Stabilizes the Tight Junction Solute Barrier through Coupling to the Perijunctional Cytoskeleton.* Molecular Biology of the Cell, 2009. **20**(17): p. 3930-3940.
52. Feldman, G.J., J.M. Mullin, and M.P. Ryan, *Occludin: Structure, function and regulation.* Advanced Drug Delivery Reviews, 2005. **57**(6): p. 883-917.
53. Krause, G., et al., *Structure and function of claudins.* Biochimica et Biophysica Acta (BBA) - Biomembranes, 2008. **1778**(3): p. 631-645.
54. Bluemel, S., et al., *The Role of Intestinal C-type Regenerating Islet Derived-3 Lectins for Nonalcoholic Steatohepatitis.* Hepatology communications, 2018. **2**(4): p. 393-406.
55. Mizoguchi, A., *Healing of intestinal inflammation by IL-22.* Inflammatory bowel diseases, 2012. **18**(9): p. 1777-1784.
56. Wang, A.-J., et al., *Genetic deletion of IL-25 (IL-17E) confers resistance to dextran sulfate sodium-induced colitis in mice.* Cell & Bioscience, 2014. **4**(1): p. 72.
57. Fatkhullina, A.R., et al., *An Interleukin-23-Interleukin-22 Axis Regulates Intestinal Microbial Homeostasis to Protect from Diet-Induced Atherosclerosis.* Immunity, 2018. **49**(5): p. 943-957.e9.
58. Fukui, A., et al., *Acetyl salicylic acid induces damage to intestinal epithelial*

cells by oxidation-related modifications of ZO-1. American journal of physiology. Gastrointestinal and liver physiology, 2012. **303**: p. G927-36.

Supplementary Table 1. The calculate table of measured mucus layer

Mucus layer thickness measured three positions (First, Second, Third) in one sample, the average value was calculated by measuring three sites at each position, and the mucus layer thickness of the sample was calculated by calculating the average value of the three positions

Group	First	Second	Third	Average
HFD 01	8.270597	7.168604	7.435232	**7.6**
HFD 02	16.65103	14.16667	18.33807	**16.4**
HFD 03	11.58453	9.446487	8.975275	**10**
HFD 04	8.549285	7.168604	8.270597	**8**
HFD 05	16.65103	19.19382	21.44923	**19.1**
HFD 06	12.11203	15.68461	16.96094	**14.9**
HFD 07	14.46363	18.43433	13.02353	**15.3**
HFD 08	10.35267	9.126856	9.623546	**9.7**
HFDB 01	20.68699	22.91667	21.86674	**21.8**
HFDB 02	30.48508	26.81275	28.17665	**28.5**
HFDB 03	18.33807	18.56389	21.8144	**19.6**
HFDB 04	23.23267	19.52562	25	**22.6**
HFDB 05	17.89728	20.63236	20.58182	**19.7**
HFDB 06	18.67578	14.58333	21.50985	**18.3**
HFDB 07	16.39889	25.5631	25.31057	**22.4**
HFDB 08	15.10381	20.03469	15.5009	**16.9**

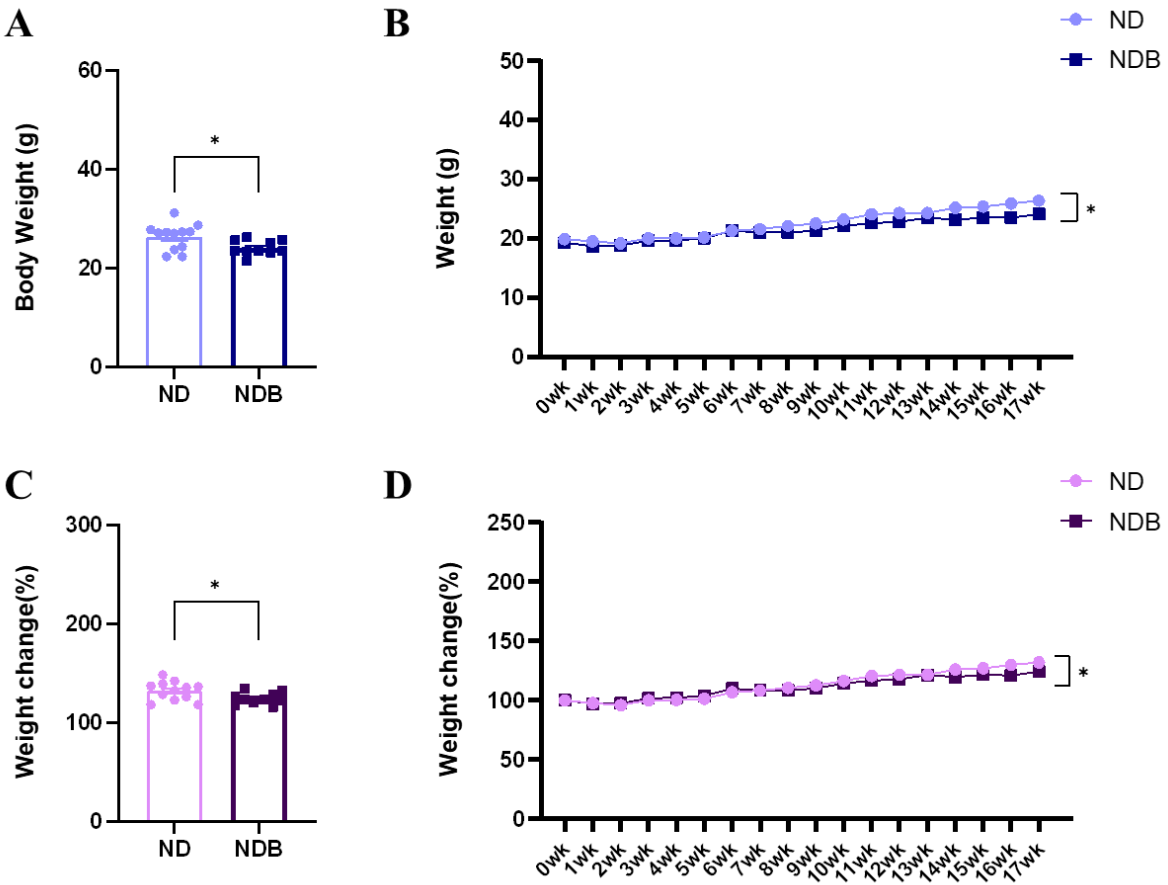
A
Body Weight (g)
60
40
20
0
*
ND
NDB
B
ND
NDB
Weight (g)
50
40
30
20
10
0
*
0wk
1wk
2wk
3wk
4wk
5wk
6wk
7wk
8wk
9wk
10wk
11wk
12wk
13wk
14wk
15wk
16wk
17wk
C
Weight change(%)
300
200
100
0
*
ND
NDB
D
ND
NDB
Weight change(%)
250
200
150
100
50
0
*
0wk
1wk
2wk
3wk
4wk
5wk
6wk
7wk
8wk
9wk
10wk
11wk
12wk
13wk
14wk
15wk
16wk
17wk

Supplementary figure 1. BV SNUG40005 slightly affects weight change in a normal diet mouse model.

All groups were given NFD for the next 18 weeks, and BV SNUG40005 and PBS were orally administered to each mouse at a concentration of 2×10^9 cfu/mouse. Weight was measured at the same time each week (A) Weight of individual mice between groups at week 18, (B) Changes in mean mouse weights between groups of mice over 18 weeks, (C) Weight change of individual mice between groups at week 18, (D) Changes in mean mouse weight change between groups of mice over 18 weeks. Each value represents each mouse. Statistical analysis was performed using a one-tailed unpaired t test based on 12 mice per group and error bars represent SEM. *, $P < 0.05$; **, $P < 0.01$; ***, $P < 0.001$.

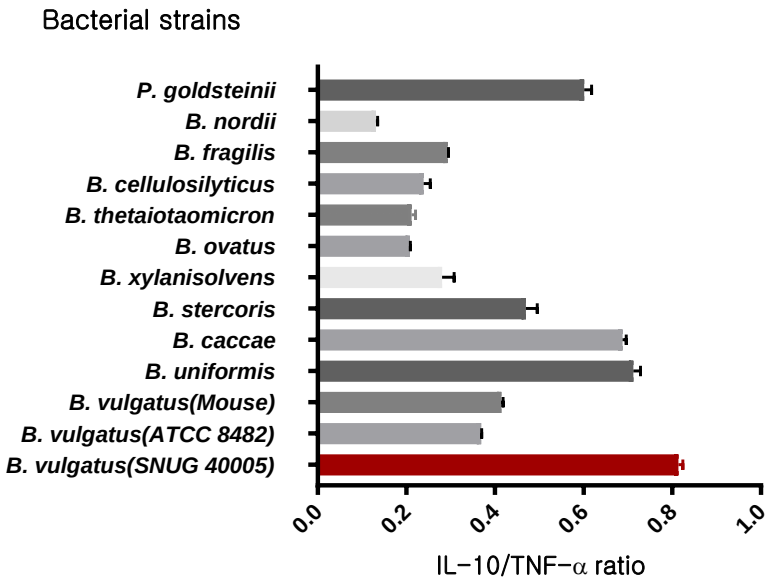

Supplementary figure 2. Isolated *Bacteroides* strains treat to human monocyte cell line THP-1 *in vitro*

Bacteroides and *Parabacteroides* species treat to THP-1 cell line. The strains used in the experiment were all isolated from healthy Korean humans, *Bacteroides vulgatus* strains were used as a strain from the ATCC, a strain isolated from the mouse, a strain isolated from human. The x-axis value indicated as the ratio of protein expression by ELISA between IL-10 and TNF-a.

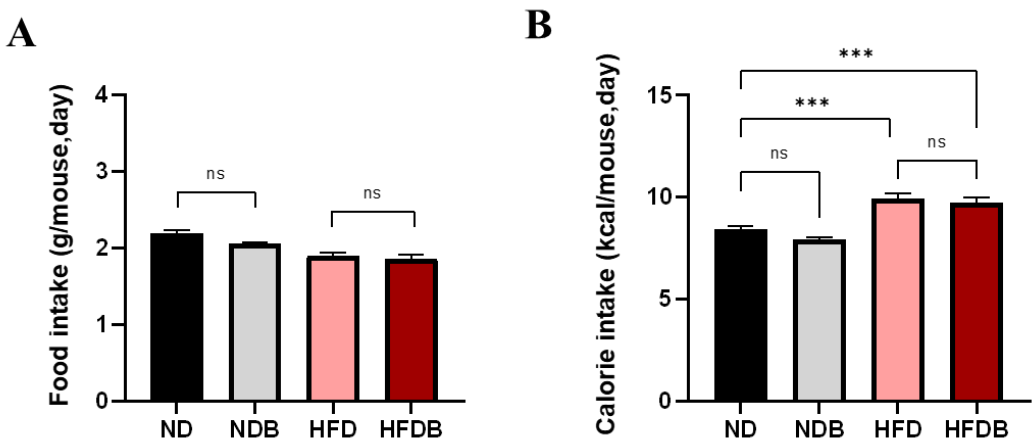

Supplementary figure 3. Daily food intake and calorie intake in each group

The food intake and calorie intake of each group were measured during the experiment. (A) In the food intake, calculated by the weight of the provided feed minus the weight of the remaining feed after one week and dividing by the number of mice. (B) For calorie intake, calculated by the food intake multiplying the calorie of the feed (The calorie of normal diets is 3.85 kcal/g, high fat diet is 5.24 kcal/g). Data shown as bar plot graph (n=8, respectively), statistical analysis was performed using a one-tailed unpaired t test and error bars represent SEM. *, $P < 0.05$; **, $P < 0.01$; ***, $P < 0.001$.

국문초록

박테로이데스 불가투스 균주의 장내 미생물 불균형 회복과 장벽 기능 개선 및 항비만 효과 연구

서울대학교 보건대학원

환경보건학과 환경보건학 전공

김진욱

지도교수 고 광 표

장내 미생물총은 비만의 발달 과정에서 면역 반응을 조절하거나, 대사의 기능저하에 중요한 역할을 한다고 알려져 있다. Firmicutes 와 Bacteroidetes 가 일반적인 성인의 두가지 우점 균주로 알려져 있으며, 이것은 사람의 비만의 척도를 나타내는 생물학적 지표로 사용된다. 박테로이데스와 비만의 상관관계는 많은 임상연구와 동물실험을 통해 보고되었지만, 그 인과관계나 작용 기전은 밝혀져 있지 않다. 본 연구에서는 고지방 식이를 통한 비만 유도 동물 모델을 이용하여, 건강한 한국인 성인으로부터 분리한 박테로이데스 균주의 항 비만효과를 연구하였다. 박테로이데스 균주는 $2x10^9$ CFU의 농도로 실험이 끝날 때까지 매일 경구 투여를 진행하였다. 고지방 식이 비만 유도 동물 모델은, 고지방 사료를 0일차부터 실험이 끝날 때까지 제공하였다. 본 실험에서, 분리한 박테로이데스 불가투스 균주의 체중 감소, 내당능 개선, 지방 조직 무게 감소, 염증 반응 감소등이 확인되었다. 또한 박테로이데스 불가투스를 투여한 마우스 그룹의 장내 미생물총에서 다양성이 증가하였으며 성상의 변화가 일어나는 것을 확인하였다. 더 나아가, 박테로이데스 불가투스 균주를 투여한 마우스 그룹에서 점액층

분비 관련 유전자 (Muc2, Muc4, Muc13, Klf4)와 장벽 기능과 관련된 유전자 (Zo-1)의 발현이 증가하는 것이 관찰되었다. 마우스의 대장 조직을 염색하여 점액층의 두께를 비교했을 때에도, 균주를 투여했을 때 유의적으로 점액층의 두께가 증가하는 것이 확인되었다. 박테로이데스 불가투스 균주의 점액 층 분비 및 장벽기능 개선 효과를 검증 하기위해, 두 종류의 사람 장벽 세포주 (LS174T, Caco-2)를 이용하여 박테로이데스 균주를 처리하고 관련유전자의 변화를 관찰하였다. 박테로이데스 불가투스 균주는 LS174T 세포주에서, 점액 층 분비 관련 유전자의 발현과, Caco-2 세포주에서 장벽 기능 관련 유전자의 발현을 증가시키는 것을 확인하였다. 이를 통해, 분리한 박테로이데스 불가투스 균주가 성공적으로 비만을 완화한다는 것을 알 수 있으며, 마이크로바이옴을 기반한 비만치료의 이용가능성을 제시할 수 있다.

주요 단어: 박테로이데스 불가투스, 비만, 비만 유도 동물, 제2형 당뇨병, 내당능, 고혈당, 장내 미생물, 마이크로바이옴, 점액 층, 장벽 기능 개선

학번: 2018-28883